Supplementary Information

$MoWS_2$ nanosheets incorporated nanocarbons for high energy density pseudocapacitive negatrode material and hydrogen evolution reaction

Abhinandan Patra[1], Monirul Shaikh[2], Saurabh Ghosh[2], Dattatray J. Late[3], Chandra Sekhar Rout[1]*

[1]Centre for Nano and Material Sciences, Jain University, Jain Global Campus, Ramanagaram, Bangalore-562112, India.

[2]Department of Physics and Nanotechnology, SRM Institute of Science and Technology, Kattankulathur 603 203, Tamil Nadu, India.

[3]Centre for Nanoscience& Nanotechnology Amity University Maharashtra, Mumbai-Pune Expressway, Bhatan, Post – Somathne, Panvel, Mumbai, Maharashtra 410206, India.

E-mail: r.chandrasekhar@jainuniversity.ac.in; csrout@gmail.com, djlate@mum.amity.edu, saurabhghosh2802@gmail.com

The capacitances calculated from CV and GCD are given below;

$$C_{s\text{-}cv} = \frac{\int Idv}{\nu \times m \times \Delta V} \quad \text{(S1)}$$

$$C_{s\text{-}GCD} = \frac{I \times \Delta T}{\Delta V \times m} \quad \text{(S2)}$$

Where I = current, ν = scan rate, m = mass loading, V = potential window, T = discharge time.

The energy density and power density are computed from the following equations[1-3];

$$E = \frac{1}{2} CV^2 \times \frac{1}{3.6} \quad \text{(S3)}$$

$$P = E/\Delta T \times 3600 \quad \text{(S4)}$$

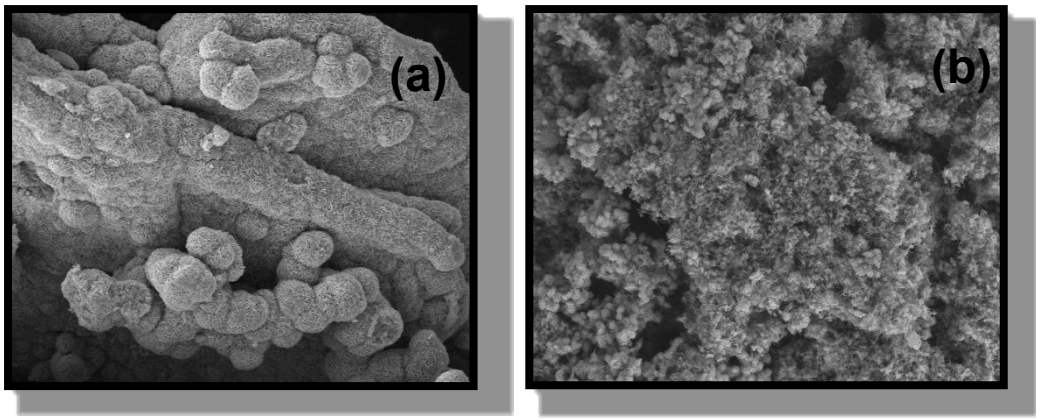

Fig-S1: FESEM images of (a) MWSR and (b) MWSC in high magnification

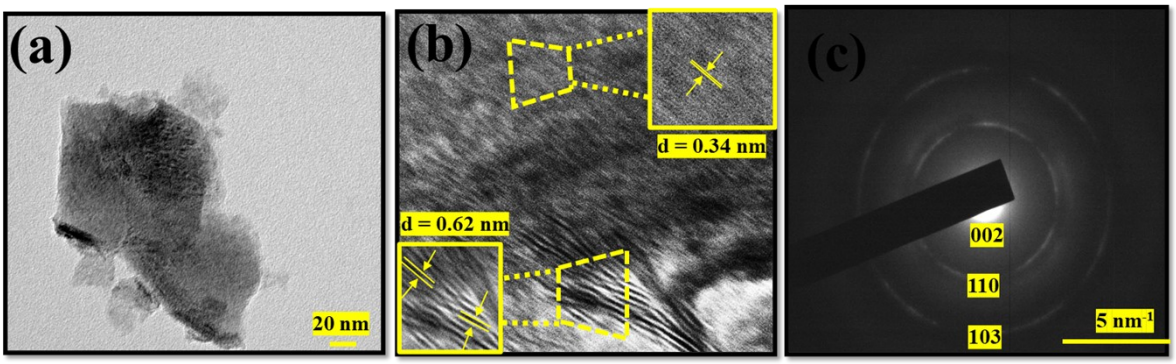

Fig-S2: TEM image of MWSR; (a)TEM image, (b) HRTEM image along with d spacing and (c) SAED pattern

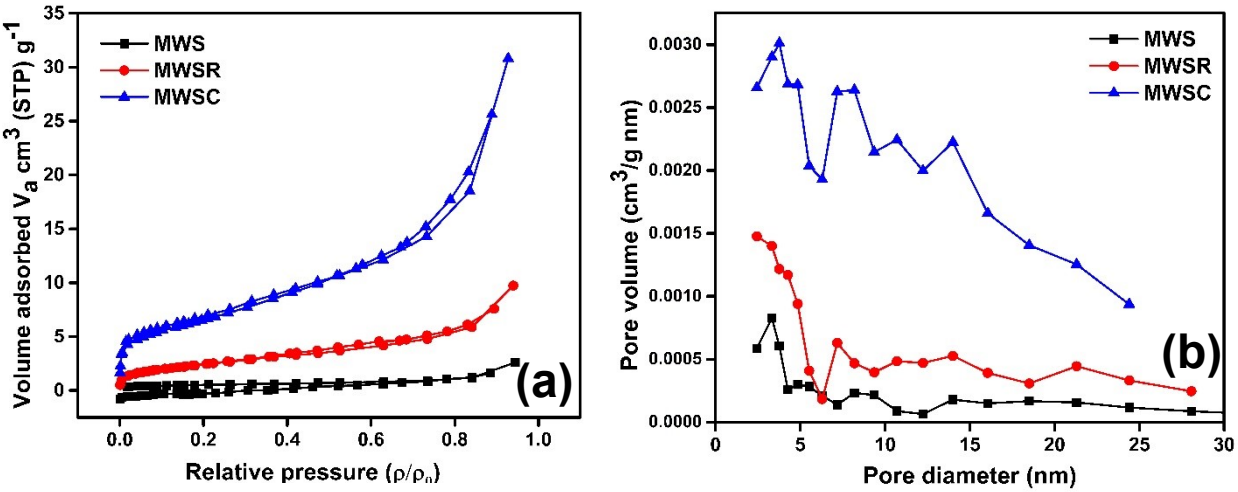

Fig-S3: Comparative **(a)** surface area characteristics and **(b)** pore size distribution of the materials collected from BET analysis

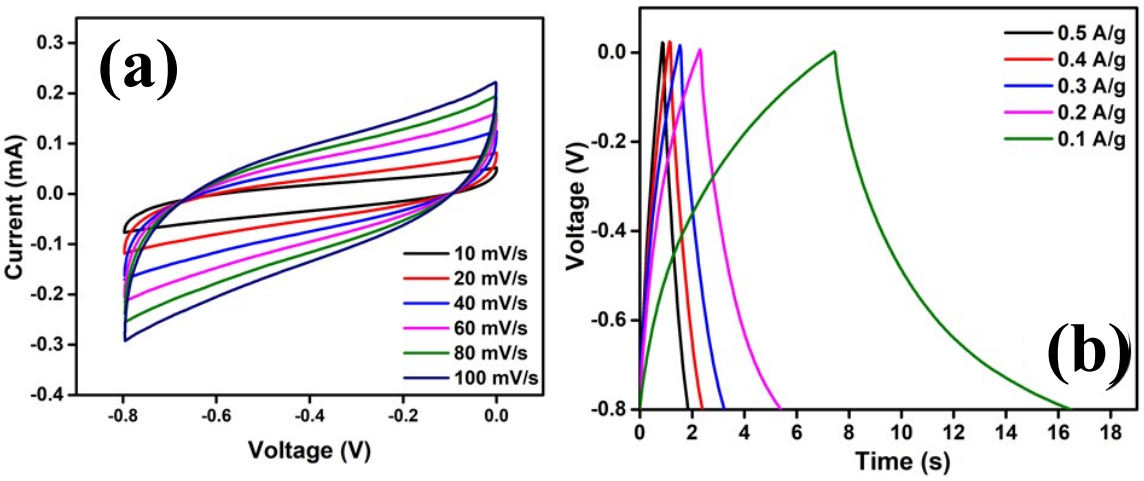

Fig-S4:(a) CVs **(b)** GCD curves of MWSC in three electrode configuration.

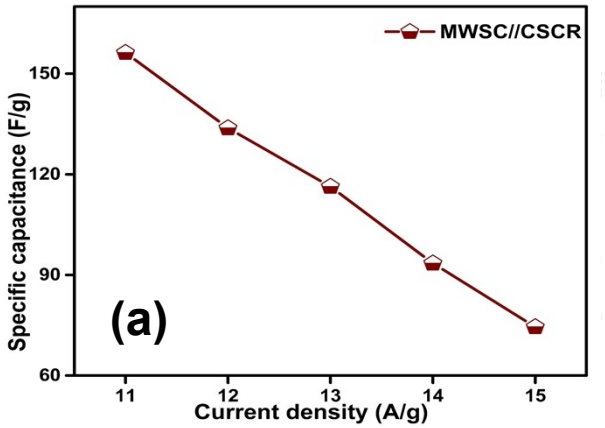

Fig-S5: (a) Specific capacitance as a function of current density of the asymmetric supercapacitor devices

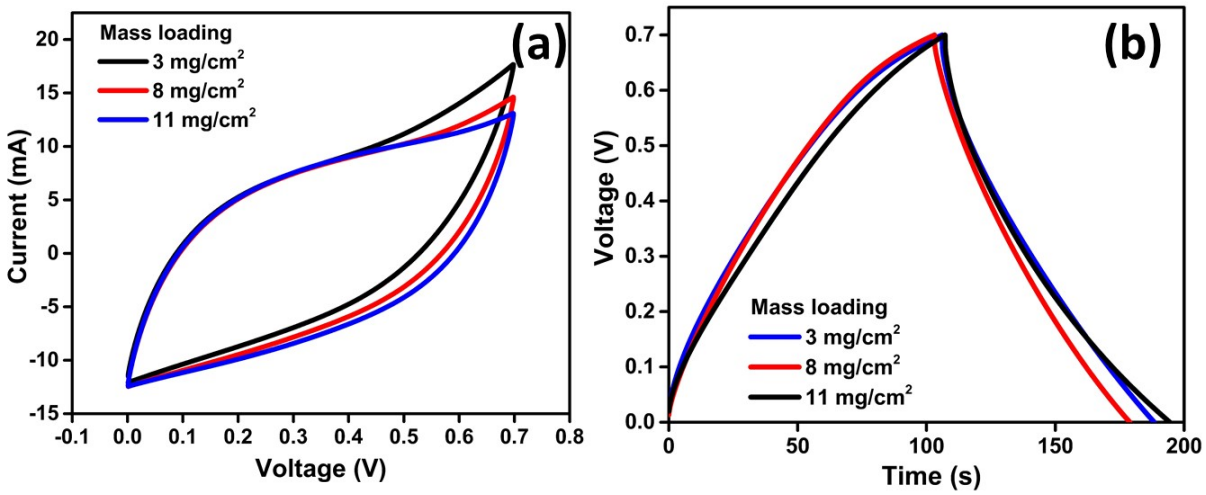

Figure S6: Performance of MWSC at higher mass loadings: (a) and (b) Comparative CV and GCD profiles

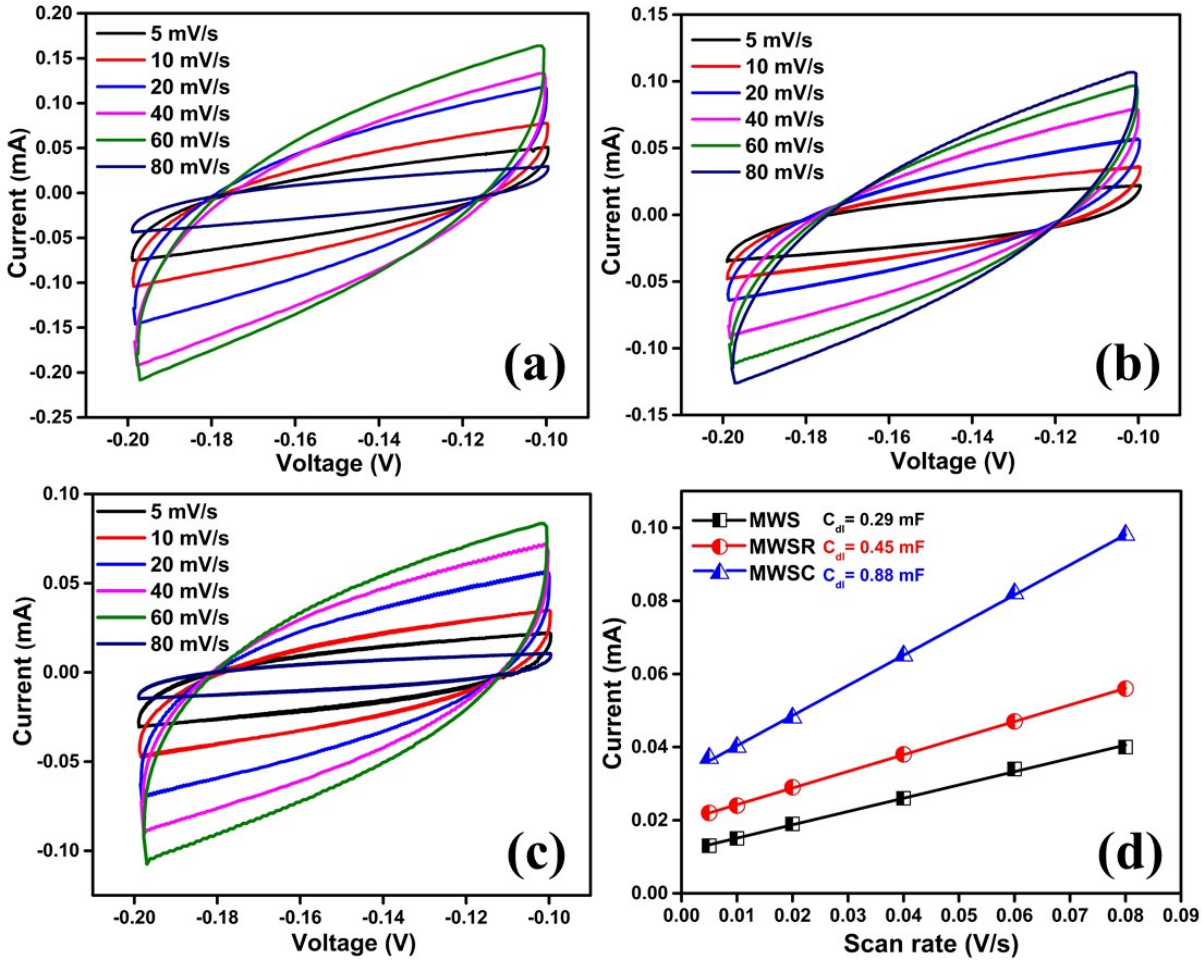

Figure S7: (a), (a), (b) and (c) illustrating the CV profiles of MWS, MWSR, MWSC at different scan rates and (d) implies the corresponding Cdl values.

Elements	Atomic percentage (%)
Mo	12.95
W	9.84
S	43.19
C	28.07
O	5.95

Table ST1: Table showing atomic percentage of MWSC calculated from XPS data confirming the presence of all the elements

Materials	Surface area (m^2/g)	Pore volume (cm^3 (STP) g^{-1})
MWS	1.586	0.364
MWSR	8.28	1.90
MWSC	23.145	5.317

Table-ST2: Surface area and pore volume values determined for MWS, MWSR and MWSC.

Materials	R_s (Solution resistance-Ω)	R_{ct} (charge transfer resistance-Ω)
MWS	2.07	9.11
MWSR	1.98	6.58
MWSC	1.69	5.06

Table-ST3: R_s and R_{ct} values calculated from EIS curves for MWS, MWSR and MWSC

Electrode materials	**Electrolyte**	**Specific capacitance (F/g)**	**Energy density (Wh/kg)**	**Power density (W/kg)**	**Capacity retention rates (%)**	**References**
MoS_2 MWCNT// PANI/MoS_2	PVA-Na_2SO_4 gel	138.13 at 1 A/g	38.9	382.61	65.2 % after 10,000 cycles	4
(rGO-MoS_2-WS_2//rGO)	KOH	48 at 0.5 A/g	15	373	70 % after 3000 cycles	5
MoS_2/NiS//AC	KOH	1493 F/g at 0.2 A/g	31	155.7	100 % after 10,000 cycles	6
MoS_2-Graphene//AEG	KOH	59 at 1 A/g	16	758	95% after 2000 cycles	7
ZIF-8 derived WS2/carbon//ZIF-8 derived carbon	H_2SO_4	88 at 1 A/g	25	800	78% after 3000 cycle	8
1T/2H-O-MoS2@GF//MnO2@GF	Na_2SO_4	88 at 0.5 A/g	39.7	450	80 % after 2000 cycles	9
$MoSTi_3C_2$/CuS//Ti_3C_2	KOH	49 at 1 A/g	15	750	82 % after 5000 cycles	10

LSG//MLSG	KOH	80 F/g at 2mV/s	142 μW h cm^{-2}	4.9 mW cm^{-2}	97 % after 10,000 cycles	11
M-$Ti_3C_2T_x$//PANI@M-Ti_3C_2T	H2SO4	87 at 1 A/g	14	127	65.2 % after 10,000 cycles	12
Ti3C2//d-Ti_3C_2/NF	KOH	51 at 0.5 A/g	18	357	81 % after 5000 cycles	13
Ni-Co-S/Co(OH)2//AC	PVA_KOH	1440.0 C/g at 1 A/g	58.4	0.8	81.4 % after 5000 cycles	14
NiCO2S4//AC	KOH	66.4 F/g at 1 A/g	27.2	0.87	80.78 % after 8000 cycles	15
L-VN@AC//α-MnO2		597.5 μWh cm^{-2} at 2.4 mW cm^{-2}	8.5 mWh cm^{-3}	34.3 mW cm^{-3}	----------	16
$MoWS_2$@MWCNT	**K_2SO_4**	**592.59 at 0.2 A/g**	**10.07**	**123.56**	**88 % after 6000 cycles**	**This work**
$MoWS_2$@MWCNT// $CoSe_2$@MWCNT@rGO	**K_2SO_4**	**118.23**	**36.67**	**14668**	**92.63% after 6000 cycles**	**This work**

Table-ST4: shows the comparison of the current work with existing literatures in the field of supercapacitor

Serial no	Electrode Material	Volumetric capacitance/capacity	References
1	1T-MoS_2/graphene	511 mAh g^{-1} 1 A g^{-1}	Yao, K., Xu, Z., Ma, M., Li, J., Lu, F. and Huang, J., 2020. Densified metallic MoS_2/graphene enabling fast potassium-ion storage with superior gravimetric and volumetric capacities. Advanced Functional Materials, 30(24), p.2001484.
2	MoS_2/CNT//MnO_2// CNT	6.5 F cm^{-3} at 10 mV/s	Tiwari, P., Janas, D. and Chandra, R., 2021. Self-standing MoS_2/CNT and MnO2/CNT one dimensional core shell heterostructures for asymmetric supercapacitor application. Carbon, 177, pp.291-303.
3	MnO_2/RGO/CF,	12 F cm^{-3} at 2 mA cm^{-2}	Zhang, Z., Xiao, F. and Wang, S., 2015. Hierarchically structured MnO_2/graphene/carbon fiber and porous graphene hydrogel wrapped copper wire for fiber-based flexible all-solid-

			state asymmetric supercapacitors. Journal of Materials Chemistry A, 3(21), pp.11215-11223.
4	PANI@CF	15 F cm^{-3} at 10 mV s-1	Jin, H., Zhou, L., Mak, C.L., Huang, H., Tang, W.M. and Chan, H.L.W., 2015. High-performance fiber-shaped supercapacitors using carbon fiber thread (CFT)@ polyanilne and functionalized CFT electrodes for wearable/stretchable electronics. Nano Energy, 11, pp.662-670.
5	MoS_2-rGO/MWCNT fiber	6 F cm^{-3} at 0.07 mA cm^{-3}	Sun, G., Zhang, X., Lin, R., Yang, J., Zhang, H. and Chen, P., 2015. Hybrid fibers made of molybdenum disulfide, reduced graphene oxide, and multi-walled carbon nanotubes for solid-state, flexible, asymmetric supercapacitors. Angewandte Chemie, 127(15), pp.4734-4739.
7	MoS_2/r-GO//Fe_2O_3/MnO_2	1.54 F/cm^3 10 mV/s	Sarkar, D., Das, D., Das, S., Kumar, A., Patil, S., Nanda, K.K., Sarma, D.D.

			and Shukla, A., 2019. Expanding interlayer spacing in MoS_2 for realizing an advanced supercapacitor. ACS Energy Letters, 4(7), pp.1602-1609.
8	MWSC	12.9 F/cm^3 at 0.06 mA/cm^3	This Work
9	CSCR//MWSC	18.6 F/cm^3 at 2.4 mA/cm^3	This Work

Table ST5: Comparison table showing the volumetric capacity/capacitance of various electrode materials

Electrocatalyst	**Electrolyte**	**Overpotential (mV)**	**Tafel slope (mV/dec)**	**References**
$MoSe_2$/Carbon cloth	H_2SO_4	200	76	17
$MoWS_2$	H_2SO_4	-	131	18
$MoWS_2$/rGO	H_2SO_4	96	38.7	19
$MoWS_2$/CNT yarn	KOH	180	46.7	20
$MoWS_2$/Carbon cloth	KOH	145	41.8	20
Tungsten doped MoS_2	H_2SO_4	165	49.3	21
$MoWS_2$@rGO	**KOH**	**243**	**68.5**	**This work**

$MoWS_2$@MWCNT	**KOH**	**175**	**54.5**	**This work**

Table-ST6: shows the comparison of the current work with existing literatures in the field of HER

REFERENCES

1 K. A. Sree Raj, A. S. Shajahan, B. Chakraborty and C. S. Rout, *Chemistry – A European Journal*, 2020, **26**, 6662–6669.

2 M. Pathak, J. R. Jose, B. Chakraborty and C. S. Rout, *The Journal of Chemical Physics*, 2020, **152**, 064706.

3 R. Samal, P. Mane, M. Bhat, B. Chakraborty, D. J. Late and C. S. Rout, *ACS Applied Energy Materials*, DOI:10.1021/acsaem.1c02205.

4 B. Cheng, R. Cheng, F. Tan, X. Liu, J. Huo and G. Yue, *Nanoscale Research Letters*, DOI:10.1186/s11671-019-2902-5.

5 T.-W. Lin, T. Sadhasivam, A.-Y. Wang, T.-Y. Chen, J.-Y. Lin and L.-D. Shao, *ChemElectroChem*, 2018, **5**, 1024–1031.

6 Q. Qin, L. Chen, T. Wei and X. Liu, *Small*, 2018, **15**, 1803639.

7 T. M. Masikhwa, M. J. Madito, A. Bello, J. K. Dangbegnon and N. Manyala, *Journal of Colloid and Interface Science*, 2017, **488**, 155–165.

8 V. Shrivastav, S. Sundriyal, V. Shrivastav, U. K. Tiwari and A. Deep, *Energy & Fuels*, 2021, **35**, 15133–15142.

9 S. Lee, J. Hwang, D. Kim and H. Ahn, *Chemical Engineering Journal*, 2021, **419**, 129701.

10 Z. Pan, F. Cao, X. Hu and X. Ji, *Journal of Materials Chemistry A*, 2019, **7**, 8984–8992.

11 L. Ma, T. Zhao, F. Xu, T. You and X. Zhang, *Chemical Engineering Journal*, 2021, **405**, 126694.

12 K. Li, X. Wang, S. Li, P. Urbankowski, J. Li, Y. Xu and Y. Gogotsi, *Small*, 2019, **16**, 1906851.

13 J. Guo, Y. Zhao, A. liu and T. Ma, *Electrochimica Acta*, 2019, **305**, 164–174.

14 X. Zhang, G. Qu, Z. Wang, G. Xiang, S. Hao, X. Wang, X. Xu, W. Ma and G. Zhao, *Chinese Chemical Letters*, 2021, **32**, 2453–2458.

15 G. Xiang, Y. Meng, G. Qu, J. Yin, B. Teng, Q. Wei and X. Xu, *Science Bulletin*, 2020, **65**, 443–451.

16 G. Qu, Z. Wang, X. Zhang, S. Zhao, C. Wang, G. Zhao, P. Hou and X. Xu, *Chemical Engineering Journal*, 2022, **429**, 132406.

17 Y. Liu, L. Ren, Z. Zhang, X. Qi, H. Li and J. Zhong, *Scientific Reports*, 2016, **6**, 22516.

18 H. Li, K. Yu, Z. Tang and Z. Zhu, *ACS Applied Materials & Interfaces*, 2016, **8**, 29442–29451.

19 Y. Lei, S. Pakhira, K. Fujisawa, X. Wang, O. O. Iyiola, N. Perea López, A. Laura Elías, L. Pulickal Rajukumar, C. Zhou, B. Kabius, N. Alem, M. Endo, R. Lv, J. L. Mendoza-Cortes and M. Terrones, *ACS Nano*, 2017, **11**, 5103–5112.

20 D. A. Nguyen, T. S. Le, D. Y. Park, D. Suh and M. S. Jeong, *ACS Applied Materials & Interfaces*, 2019, **11**, 37550–37558.

21 Q. Xu, Y. Zhang, Y. Zheng, Y. Liu, Z. Tian, Y. Shi, Z. Wang, J. Ma and W. Zheng, *The Journal of Physical Chemistry C*, 2021, **125**, 11369–11379.